APPLIED PHYSICS

Electric dipole effect in $PdCoO_2/\beta\text{-}Ga_2O_3$ Schottky diodes for high-temperature operation

T. Harada[1]*, S. Ito[1], A. Tsukazaki[1,2]

High-temperature operation of semiconductor devices is widely demanded for switching/sensing purposes in automobiles, plants, and aerospace applications. As alternatives to conventional Si-based Schottky diodes usable only at 200°C or less, Schottky interfaces based on wide-bandgap semiconductors have been extensively studied to realize a large Schottky barrier height that makes high-temperature operation possible. Here, we report a unique crystalline Schottky interface composed of a wide-gap semiconductor $\beta\text{-}Ga_2O_3$ and a layered metal $PdCoO_2$. At the thermally stable all-oxide interface, the polar layered structure of $PdCoO_2$ generates electric dipoles, realizing a large Schottky barrier height of ~1.8 eV, well beyond the 0.7 eV expected from the basal Schottky-Mott relation. Because of the naturally formed homogeneous electric dipoles, this junction achieved current rectification with a large on/off ratio approaching 10^8 even at a high temperature of 350°C. The exceptional performance of the $PdCoO_2/\beta\text{-}Ga_2O_3$ Schottky diodes makes power/sensing devices possible for extreme environments.

INTRODUCTION

Recent requirements for Schottky junctions are demanding, particularly for switching/sensing device applications under harsh operating conditions, including high current densities, frequencies, and temperatures (*1*, *2*). However, conventional Si-based Schottky diodes suffer from serious current leakage at more than 200°C because of the small Schottky barrier height (~0.9 eV) limited by the narrow bandgap of Si (~1.1 eV) (*1*). To realize a higher-temperature operation, alternative Schottky interfaces with a large Schottky barrier height should be developed on the basis of wide-bandgap semiconductors. The energy barrier height ϕ_b is shown in an ideal band diagram for a metal-semiconductor Schottky interface (Fig. 1A) according to the Schottky-Mott relation: $\phi_b = \phi_m - \chi_s$, where ϕ_m is the work function of a metal and χ_s is the electron affinity of the semiconductor (*3*). The typical rectifying current-voltage characteristics of a Schottky junction, schematically shown in Fig. 1B, can be formulated by a simple thermionic emission model, as in Eq. 1.

$$J = A^{**}T^2 e^{-(\phi_b/k_B T)}\left[e^{(qV/nk_B T)} - 1\right] \tag{1}$$

where J is the current density, A^{**} is the effective Richardson constant, T is the absolute temperature, q is the elementary charge, k_B is the Boltzmann constant, n is the empirical ideality factor, and V is the applied bias voltage. The ideal reverse current density J_s (J is for $V < 0$) is defined as the saturation value $J_s = A^{**}T^2 e^{-(\phi_b/k_B T)}$, as highlighted in Fig. 1B, providing the fundamental lower bound of the reverse current density achievable at a given temperature (*1*). The benchmark for high-temperature operation of Schottky diodes is exemplified by the temperature dependence of J_s at $\phi_b = 1.0$, 1.4, and 1.8 eV (Fig. 1C). For high-temperature operation, the thermally excited J_s must be suppressed by a large barrier height to achieve a large on/off ratio together with high forward current. For example, a ϕ_b >1.4 eV is required to maintain J_s below 10^{-6} A/cm^2 at 250°C, which is a typical temperature in automobile engines.

Semiconductors that are capable of realizing a high ϕ_b, beyond 1.4 eV, include wide-bandgap materials, such as SiC, GaN, and Ga_2O_3 (*4*). In particular, Ga_2O_3 devices have recently attracted considerable attention owing to their wide bandgap of approximately 5 eV, the high-temperature stability of the material, and commercial availability of large single crystals (*5*). Diode operation has been demonstrated in Schottky junctions, composed of polycrystalline Pt (*6*, *7*) and Ni (*6*, *8*–*10*) and oxidized metals (*11*–*13*) (see table S1 for polycrystalline metals and table S2 for oxidized metals). The finite range of available work functions in elemental metal electrodes, 4.0 to 5.6 eV (*14*), limits the achievable Schottky barrier height in the Schottky-Mott framework: $\phi_b = \phi_m - \chi_s$. For stable operation, choosing a thermally stable Schottky contact is crucial to avoid interfacial reactions and maintain the ϕ_b value at high temperature (*15*).

Rather than using the polycrystalline electrodes, we chose a crystalline interface, where a metal is rigidly integrated with a semiconductor. To achieve a large Schottky barrier height beyond the limitation of the Schottky-Mott rule, we used a polar interface of oxide heterostructures, combining Ga_2O_3 with a polar layered metal $PdCoO_2$ (Fig. 1D). The layered delafossite structure of $PdCoO_2$ with alternating Pd^+ and $[CoO_2]^-$ sublattices has two remarkable features (*16*, *17*): an out-of-plane polarity and high in-plane conductivity (*18*–*20*). The out-of-plane polarity, given by the alternating charged Pd^+ and $[CoO_2]^-$ sublattices of $PdCoO_2$, has recently been revealed to modulate the surface physical properties of $PdCoO_2$ bulk single crystals (*21*, *22*). This polar ionic stacking can effectively induce an electric dipole layer that enhances the Schottky barrier height at the interface. The high in-plane conductivity of $PdCoO_2$, comparable to that of Au, supports its applicability as a Schottky contact metal. The hexagonal lattice oxygen atoms on the surface of $PdCoO_2$ (0001) match those of $\beta\text{-}Ga_2O_3$ (−201), which makes it possible to form a functional interface that leverages the polar nature of $PdCoO_2$.

RESULTS

We fabricated heterostructures of 20-nm-thick $PdCoO_2/\beta\text{-}Ga_2O_3$ (a commercial n-type substrate with a nominal donor density of 7.8×10^{17} cm^{-3}) by pulsed-laser deposition. The *c* axis–oriented growth was observed in typical x-ray diffraction patterns (fig. S1A). The

---

[1] Institute for Materials Research, Tohoku University, Sendai 980-8577, Japan.
[2] Center for Spintronics Research Network (CSRN), Tohoku University, Sendai 980-8577, Japan.
*Corresponding author. Email: t.harada@imr.tohoku.ac.jp

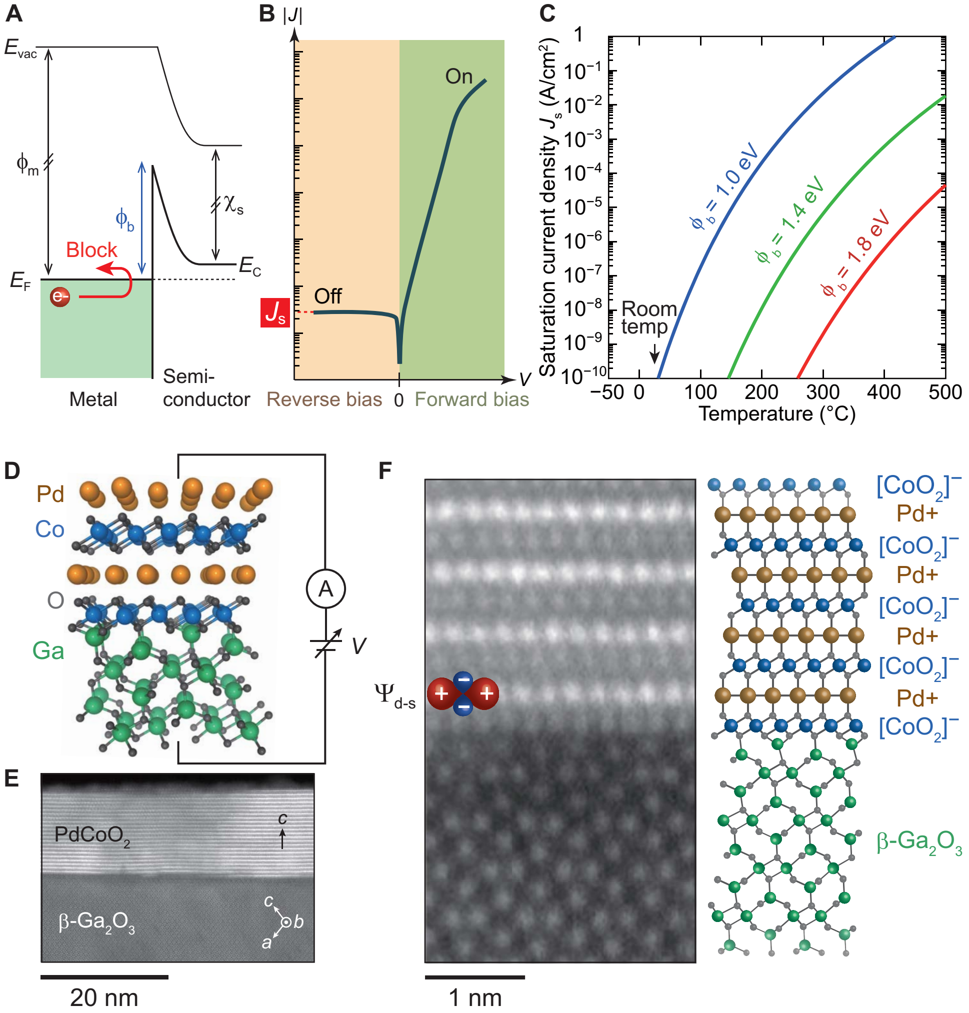

Fig. 1. Schottky junctions based on a layered $PdCoO_2$ and β-Ga_2O_3 for high-temperature operation. (**A**) Energy band diagram of a metal-semiconductor interface with a Schottky barrier of ϕ_b. ϕ_m, work function of metal; χ_s, electron affinity of semiconductor; E_{vac}, vacuum level; E_F, Fermi energy; E_C, conduction band minimum; V, bias voltage. The electron is depicted as a red circle. (**B**) Typical current-voltage characteristic of Schottky junction showing the current rectification behavior under forward (on-state) or reverse (off-state) bias voltage. The saturation current density J_s is noted in red. (**C**) Temperature dependence of the saturation current density J_s with Schottky barrier heights of 1.0 eV (blue), 1.4 eV (green), and 1.8 eV (red) calculated by the thermionic emission model using the Richardson constant of β-Ga_2O_3, $A^{**} = 41.1$ A/cm^2 (*24*). (**D**) Schematic image for the characterization of the $PdCoO_2$/–β-Ga_2O_3 Schottky junction. (**E**) HAADF-STEM image of the $PdCoO_2$/β-Ga_2O_3 interface. The crystal orientation is represented by arrows. (**F**) Enlarged image of the HAADF-STEM image of the $PdCoO_2$/β-Ga_2O_3 interface. The anisotropic $\Psi_{d\text{-}s}$ orbital proposed for the conduction band of $PdCoO_2$ is schematically shown (*20*). Right: Corresponding crystal model. The alternating Pd^+ and $[CoO_2]^-$ charged layers are shown based on the nominal ionic charges in the bulk $PdCoO_2$. The actual charge state at the interface can be modified by electronic reconstruction with screening charges.

lattice arrangement at the interface was imaged with a high-angle annular dark-field scanning transmission electron microscope (HAADF-STEM), as shown in Fig. 1 (E and F). The layered crystal structure of $PdCoO_2$ was seen, and no threading dislocations were apparent (Fig. 1E), indicating an epitaxial relationship of $PdCoO_2$ [0001]//β-Ga_2O_3 [−201], although the in-plane lattice mismatch was large at approximately 3%, as estimated from the O-O distances of 2.83 Å for $PdCoO_2$ and 2.93 Å for β-Ga_2O_3 (fig. S2). An enlarged HAADF-STEM image (Fig. 1F) shows that the $[CoO_2]^-$ layer corresponds to the initial layer of $PdCoO_2$ on the β-Ga_2O_3. The wave function of the Pd^+ conducting layer is depicted in the inset of Fig. 1F, producing a polar interface between $PdCoO_2$/β-Ga_2O_3 and the highly anisotropic in-plane conductivity in $PdCoO_2$. The in-plane conductivity of the $PdCoO_2$/β-Ga_2O_3 is approximately 6.3×10^4 S/cm at room temperature (fig. S1B), the value of which is high enough to achieve sufficient current spreading in the contact pad. Here, only the polarity originating from the $PdCoO_2$ layer is considered, because the β-Ga_2O_3 (−201) surface is likely to be reconstructed to a stable nonpolar structure before the $PdCoO_2$ deposition. The abrupt interface of $PdCoO_2$/β-Ga_2O_3 provides a suitable platform for exploiting interfacial dipole effects with minimized extrinsic contributions, i.e., defects.

To investigate the Schottky characteristics of the $PdCoO_2$/β-Ga_2O_3 junctions, we patterned the $PdCoO_2$ thin films into circle-shaped devices using a water-soluble templating process (*23*). Typical *J-V* characteristics (Fig. 2A) showed clear rectification with a resistance ratio $>10^9$ and a reverse current density as low as the measurement limit of 10^{-8} A/cm^2 at 220°C (blue). Applying Eq. 1 to the forward-bias region made it possible to evaluate the Schottky barrier height ϕ_b (the symbol

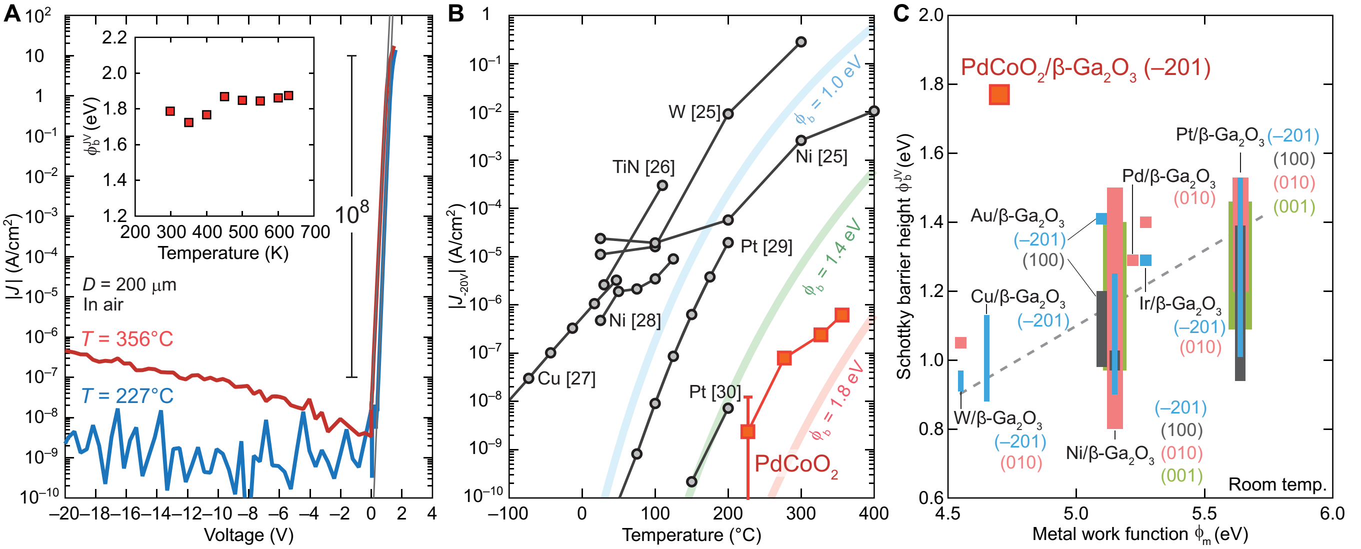

Fig. 2. High-temperature operation of the $PdCoO_2$/β-Ga_2O_3 Schottky junctions with a large barrier height. (**A**) Current-voltage characteristics of the $PdCoO_2$/β-Ga_2O_3 Schottky junction with a diameter of 200 μm at 227°C (blue) and 356°C (red). The gray lines are the linear fitting for the forward-bias region. The temperature dependence of the Schottky barrier height is plotted in the inset. (**B**) Temperature-dependent reverse current density under the bias voltage of −20 V $|J_{-20V}|$ plotted together with the reported values (*25*–*30*). The ideal J_s in Fig. 1C is also shown for ϕ_b = 1.0 eV (blue), 1.4 eV (green), and 1.8 eV (red). (**C**) Comparison of the Schottky barrier height with the reported values for elemental metal Schottky junctions (see the Supplementary Materials for the data and references used). Perpendicularly spread line data correspond to the range of the reported Schottky barrier height. The different colors correspond to the different surface orientations of the β-Ga_2O_3 layers. The linear trend from the reported values is shown as a broken line. The large red square corresponds to the data obtained for $PdCoO_2$/β-Ga_2O_3.

ϕ_b^{JV} is used to specify the measurement technique: *J*-*V* measurement) and the ideality factor *n*, which were approximately 1.85 eV and 1.04, respectively, at 220°C, using the A^{**} = 41.1 A/cm² of β-Ga_2O_3 (*24*). These values are close to the corresponding values of 1.78 eV and 1.06 characterized at room temperature. Such rectifying properties were maintained at 350°C (Fig. 2A, red) together with a large on/off ratio of approximately 10^8 and a reverse current density of 10^{-6} A/cm². Moreover, the weak temperature dependences of ϕ_b^{JV} (inset of Fig. 2A) and the ideality factor (fig. S3A) indicate the homogeneous Schottky barrier height at the interface (see Materials and Methods for a detailed discussion). The value of ϕ_b^{JV} is mainly dominated by the activation process across the lowest-energy barrier region. The reverse current density (V = −20 V) at high temperature (Fig. 2B) is compared with the ideal J_s lines (Fig. 1C) and data from previous studies (*25*–*30*). Owing to the large ϕ_b^{JV}, the value of $|J_{-20V}|$ at the $PdCoO_2$/β-Ga_2O_3 junction (Fig. 2B, red squares) is suppressed at the measured high temperatures. We compare our ϕ_b^{JV} values with metal/β-Ga_2O_3 junctions of previous studies (table S1), where ϕ_b^{JV} is plotted as a function of the metal work function ϕ_m (Fig. 2C). The large deviation of the reported ϕ_b^{JV} values for the specific metal/β-Ga_2O_3 junctions probably arises because of the differences in interface quality, e.g., a partial Fermi-level pinning at the surface that can occur (*31*), even when the same metal contacts are used. As measured by ultraviolet photoelectron spectroscopy (fig. S4), the $PdCoO_2$ film is plotted at a work function of 4.7 eV in Fig. 2C. The ϕ_b^{JV} value of 1.8 eV for $PdCoO_2$/β-Ga_2O_3 is located above the empirical trend of the reported values in the elemental metal/β-Ga_2O_3 junctions (gray dotted line), whose barrier height lies in the range of 1.0 to 1.5 eV (table S1). Although partial oxidation of metals is known to increase ϕ_b^{JV} (*11*–*13*), the work function and crystal structures/orientations are unknown for the oxidized states of the polycrystalline film. The plot shown in Fig. 2C, which is based on the experimentally determined values of ϕ_b^{JV} and ϕ_m, indicates that ϕ_b^{JV} of $PdCoO_2$/β-Ga_2O_3 is strongly influenced by the interfacial effects existing at the abrupt interface with well-defined crystal orientation, as shown in Fig. 1 (E and F).

In addition to the *J*-*V* characteristics, we performed capacitance (C) measurements $1/C^2 - V$ (Fig. 3A) to determine the Schottky barrier height at the interface. The gradients of linear fits to the data in Fig. 3A for two device sizes (diameter D = 100 and 200 μm) indicate that the built-in potential at the Ga_2O_3 qV_{bi} and the donor density N_D are 2.0 eV and 3×10^{17} cm^{-3}, respectively. This N_D value is comparable to the nominal donor concentration of a commercial substrate. The junction capacitance measured with V = 0 V is independent of the AC frequency (f) over a broad range from 10^2 to 10^6 Hz, with a negligible deep trap-state capacitance $C_{trap}(f)$ (inset of Fig. 3B), which suggests the potential application of this junction in high-frequency switching elements.

The band diagram for the $PdCoO_2$/β-Ga_2O_3 interface is depicted in Fig. 3C based on the experimental characteristics discussed above. First, the Schottky-Mott relation, $\phi_b = \phi_m - \chi_s$, was adopted to estimate ϕ_b to be approximately 0.7 eV, based on the work function ϕ_m for $PdCoO_2$ (4.7 eV; fig. S4) and the reported electron affinity χ_s of β-Ga_2O_3 (4.0 eV) (*32*). Although minor effects, such as energy lowering by an image force at the interface and the Fermi energy in Ga_2O_3, might make an additional contribution to the estimated value of ϕ_b (see Materials and Methods), it is difficult to explain the large mismatch between 0.7 eV and the experimentally evaluated result of 1.8 eV. As shown in Fig. 3C, the vacuum level shifted by $\Delta \approx 1.1$ eV, which contributed to the large ϕ_b^{JV}. This shift is attributed to the polar nature of $PdCoO_2$, which is composed of Pd^+ and $[CoO_2]^-$. The formation of a polar interface $[CoO_2]^-/Ga_2O_3$ (STEM image in Fig. 1F and bottom of Fig. 3C) caused ϕ_b to increase to 1.8 eV through electric dipole effects. The interface dipole caused by the $PdCoO_2$ polar layered structure agrees well with the calculated surface potential at O- and

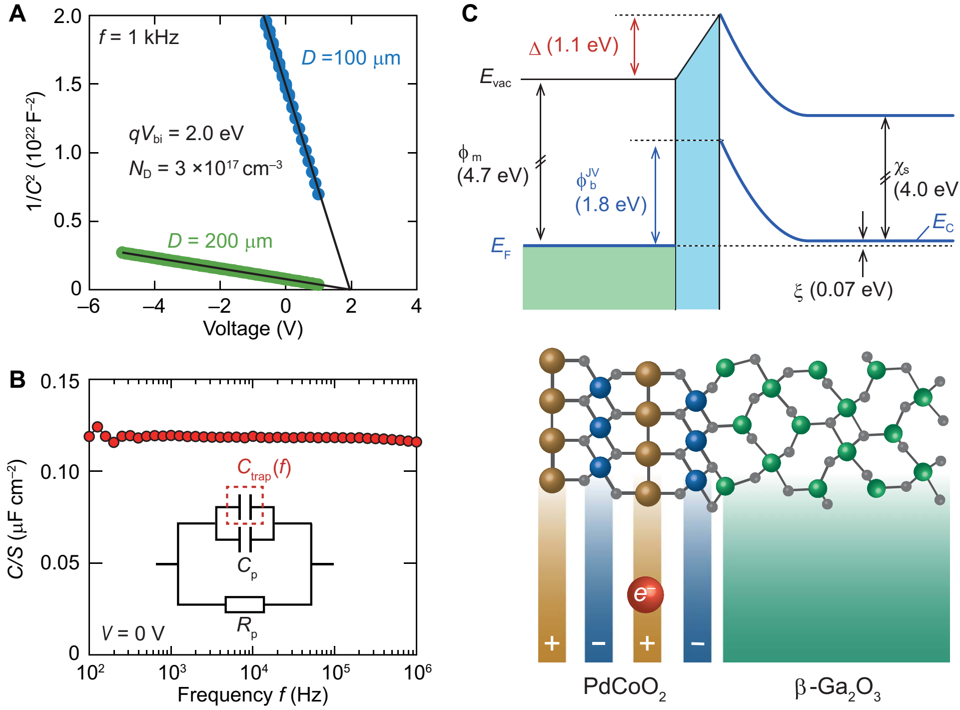

Fig. 3. Energy band diagram of the $PdCoO_2$/β-Ga_2O_3 interface. (**A**) $1/C^2$-V plots for the devices with D = 100 and 200 μm measured with an AC frequency of 1 kHz at room temperature. (**B**) Frequency dependence of the capacitance measured with 0.1-V excitation. (**C**) Top: Band diagram for the $PdCoO_2$/β-Ga_2O_3 Schottky junction based on experimentally observed values. The energy difference of the conduction band bottom and the Fermi energy in β-Ga_2O_3 (ξ) is calculated using $\xi = k_BT\ln(N_C/N_D)$ and $N_C = 2(2\pi m^* k_BT/h^2)^{3/2}$, where h is the Planck constant and $m^* = 0.342m_0$ is the effective mass of the electron in β-Ga_2O_3 (*24*). Bottom: Schematics of the $PdCoO_2$/β-Ga_2O_3 interface. A conduction electron in the Pd^+ layer is shown in red. The bulk-like charged layers of $PdCoO_2$ are schematically depicted, neglecting possible charge reconstructions.

Pd-terminated PdO (111), which predicts an energy shift of 1.2 eV (*33*). The contributions of this interfacial dipole model to $\phi_b{}^{JV}$ are analogous to the barrier height control achieved in $SrRuO_3$/Nb:$SrTiO_3$ Schottky junctions by the insertion of $[AlO_2]^-$ or $[LaO]^+$, which increase and decrease, respectively, the Schottky barrier height from its original level at ~1.3 eV to 1.8 and 0.7 eV (*34*). In the $PdCoO_2$/β-Ga_2O_3 interfaces, the interface dipole is naturally activated owing to the unique polar layered structure and the $[CoO_2]^-$ initial layer favored by the crystal growth of $PdCoO_2$ electrodes (Fig. 1F).

We examined the uniformity and reproducibility of the junction properties by measuring arrays of $PdCoO_2$ circular devices on β-Ga_2O_3 with various junction areas (from 100 to 1000 μm), as shown in the sample picture (Fig. 4A). A large $\phi_b{}^{JV}$ of approximately 1.8 eV was obtained, irrespective of the diameter of the devices (Fig. 4B). This result contrasts with the expected inhomogeneous $\phi_b{}^{JV}$ in typical large Schottky junctions owing to the high probability of pinhole-generating regions. Moreover, 27 devices were characterized with D = 100 μm to confirm the uniformity of operation. The J-V data were consistent, as shown in Fig. 4C. A histogram of $\phi_b{}^{JV}$ indicated a reproducible value of $\phi_b{}^{JV}$ = 1.76 eV with a narrow distribution of approximately 0.045 eV. Unlike the broad distribution of $\phi_b{}^{JV}$ values for the polycrystalline metal/β-Ga_2O_3 junction, as summarized in Fig. 2C, the highly reproducible $\phi_b{}^{JV}$ could result from the layered structural features and the all-oxide high-quality interface with the homogeneous $[CoO_2]^-$/Ga_2O_3 polar stacks energetically favored during the thin-film growth (Fig. 1, E and F). Hexagonal interfaces of layered $PdCoO_2$ on other semiconductors, such as SiC and GaN, could also benefit from this interfacial electric dipole effect.

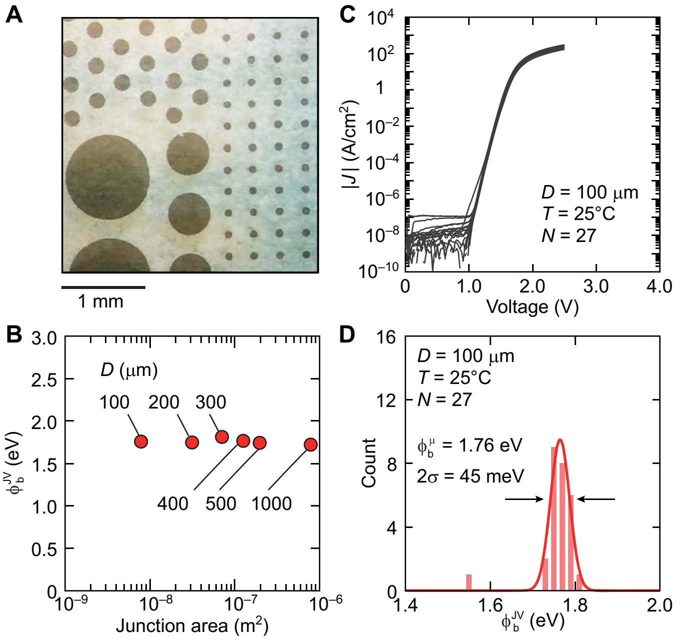

Fig. 4. Uniformity and reproducibility of the large barrier height in the $PdCoO_2$/β-Ga_2O_3 Schottky junctions. (**A**) Optical microscopy image of the $PdCoO_2$/β-Ga_2O_3 Schottky junction arrays. (**B**) Schottky barrier height obtained for the devices with different junction sizes. (**C**) Current-voltage characteristics of the 27 different devices. (**D**) Histogram of the Schottky barrier height for D = 100-μm devices. The Gaussian fitting (red curve) gives the central value $\phi_b{}^{\mu}$ = 1.76 eV and the width of distribution 2σ = 45 meV, where σ is the SD.

DISCUSSION

Superior Schottky junction properties were demonstrated with large on/off ratios, high-temperature operation at 350°C, no dependence of *C-f* characteristics, and considerable uniformity and reproducibility. This performance is attributed to the large $\phi_b{}^{JV}$ induced by the naturally formed electric dipoles at the well-regulated polar oxide interface of $PdCoO_2$ and β-Ga_2O_3. For applications under harsh conditions, $PdCoO_2$ electrodes have considerable advantages owing to their exceptional stability to heat (~800°C), chemicals (acids/bases, pH 0 to 14), and mechanical stress (fig. S5), in addition to high optical transparency (*35*). The abrupt interface of the layered oxides $PdCoO_2$ and β-Ga_2O_3 can extend applications of semiconductor devices to hot operating environments, such as those in automobile and aerospace applications.

MATERIALS AND METHODS

Substrate preparation

For the devices with acid-cleaned β-Ga_2O_3, commercially available unintentionally doped β-Ga_2O_3 (−201) substrates with the nominal $N_D = 7.8 \times 10^{17}$ cm^{-3} (Novel Crystal Technology Inc.) were immersed in an acidic solution (water: 30 to 35.5%; H_2O_2: 95%; H_2SO_4 = 1:1:4) for 5 min, followed by rinsing in water for 15 min.

$PdCoO_2$/β-Ga_2O_3 device fabrication

To pattern the $PdCoO_2$ layer by soft lithography, we used the $LaAlO_3/BaO_x$ template as a water-soluble sacrificial layer (*23*). First, an organic photoresist was patterned on the β-Ga_2O_3 substrates using a standard photolithography process. The $LaAlO_3$ (~40 nm)/BaO_x (~100 nm) templates were then deposited by pulsed-laser deposition at room temperature under the base pressure of ~10^{-7} torr. Removing organic photoresist by hot acetone gave the patterned $LaAlO_3/BaO_x$ template on the β-Ga_2O_3 substrates. Just before the deposition of $PdCoO_2$ thin films, the $LaAlO_3/BaO_x$/β-Ga_2O_3 samples were put in O_2 plasma for 50 s to remove the residual photoresist. The $PdCoO_2$ thin films were grown by pulsed-laser deposition (*35*) at a growth temperature of 700°C and an oxygen partial pressure of 150 mtorr. A KrF excimer laser was used to alternately ablate the $PdCoO_2$ stoichiometric target and Pd-PdO mixed phase target. After the thin-film growth, the $LaAlO_3/BaO_x$ templates were removed by sonication in water together with the unnecessary parts of the $PdCoO_2$ to obtain the circular $PdCoO_2$ electrodes with a diameter of 100 to 1000 μm.

Electrical transport measurement

Current-voltage characteristics of the Schottky junctions were measured via two-wire configuration using a Keithley 2450 source meter. Al wires were bonded to the top surface of the β-Ga_2O_3 substrates to form ohmic contacts to the β-Ga_2O_3 substrates. A needle prober was used to contact the $PdCoO_2$ and Pt top electrodes for the room temperature measurement. The capacitance measurements were carried out using an Agilent E4980A precision LCR meter with an AC modulation voltage of 0.1 V. The resistivity of the $PdCoO_2$ thin films was measured using a four-probe configuration.

Effect of image force lowering

For the interface of a metal and an n-type semiconductor with the relative permittivity of ε_r, the image force lowering Δϕ under zero bias can be formulated as

$$\Delta\phi = q\{q/4\pi\varepsilon_r\varepsilon_0[2qV_{\mathrm{bi}}N_D/\varepsilon_r\varepsilon_0]^{1/2}\}^{1/2}$$

Here, ε_0 is the vacuum permittivity. Using the experimentally determined qV_{bi} and N_D for the $PdCoO_2$/β-Ga_2O_3, qV_{bi} = 2.0 eV and $N_D = 3 \times 10^{17}$ cm^{-3}, and the reported ε_r = 10 (*36*), Δϕ was estimated to be 0.08 eV.

Estimation of the spatial homogeneity of the Schottky barrier height

We analyzed the temperature-dependent Schottky barrier height and the ideality factor using the potential fluctuation model to estimate the homogeneity of the barrier height (*37*). We considered the spatial distribution of the Schottky barrier height (ϕ_b) and the built-in potential (V_{bi}) by introducing the Gaussian distribution $P(qV_{\mathrm{bi}})$ and $P(\phi_b)$, with an SD σ_s around the mean values $\bar{V}_{\mathrm{bi}}$ and $\bar{\phi}_b$.

$$P(\phi_b) = \frac{1}{\sigma_s\sqrt{2\pi}}e^{-(\bar{\phi}_b-\phi_b)^2/(2\sigma_s{}^2)} \quad (2)$$

$$P(qV_{\mathrm{bi}}) = \frac{1}{\sigma_s\sqrt{2\pi}}e^{-(q\bar{V}_{\mathrm{bi}}-qV_{\mathrm{bi}})^2/(2\sigma_s{}^2)} \quad (3)$$

As discussed by Werner and Güttler (*37*), the Schottky barrier height determined by the current-voltage characteristic, $\phi_b{}^{JV}$, relates to the $\bar{\phi}_b$ and σ_s as

$$\phi_b^{JV} = \bar{\phi}_b - \frac{\sigma_s^2}{2k_BT} \quad (4)$$

Capacitance-voltage (*C-V*) measurement probes the spatial average of the built-in potential, $V_{\mathrm{bi}}{}^{CV} = \bar{V}_{\mathrm{bi}}$, which relates to the Schottky barrier height $\phi_b{}^{CV}$ to be

$$\phi_b^{CV} = q\bar{V}_{\mathrm{bi}} + k_BT\ln(N_C/N_D) = \bar{\phi}_b \quad (5)$$

where N_C and N_D denote the effective density of states in the conduction band and the doping concentration, respectively. Here, we neglected a possible contribution from the image force in the calculation of $\phi_b{}^{CV}$, which did not change the estimation of σ_s.

Comparing Eqs. 4 and 5, we found

$$\phi_b^{CV} - \phi_b^{JV} = \frac{\sigma_s^2}{2k_BT} \quad (6)$$

We fitted the experimental data by Eq. 6, as shown in fig. S3B, to obtain the SD σ_s = 54 meV, which is less than half of the reported value for Pt/β-Ga_2O_3 (σ_s = 130 meV) (*38*). The ideality factor $n(V,T)$ reflects the voltage-dependent mean barrier $\bar{\phi}_b(V)$ and the SD $\sigma_s^2(V)$ as

$$n^{-1}(V,T) - 1 = -\frac{\bar{\phi}_b(V) - \bar{\phi}_b(0)}{qV} + \frac{\sigma_s{}^2(V) - \sigma_s(0)^2}{2k_BTqV}$$

Assuming that $\bar{\phi}_b(V)$ and $\sigma_s{}^2(V)$ vary linearly with the bias voltage *V*, we can parameterize the voltage deformation of the barrier distribution using the coefficients ρ_2 and ρ_3.

$$\bar{\phi}_b(V) - \bar{\phi}_b(0) = \rho_2 qV$$

$$\sigma_s^{\,2}(V) - \sigma_s(0)^2 = \rho_3 qV$$

$$n^{-1}(T) - 1 = -\rho_1(T) = -\rho_2 + \frac{\rho_3}{2k_B T} \qquad (7)$$

The experimental data for the $PdCoO_2$/β-Ga_2O_3 Schottky junction are fitted by Eq. 7, as shown in fig. S3C, to obtain the temperature-independent coefficients $\rho_2 = -0.073$ and $\rho_3 = -1.93$ meV.

SUPPLEMENTARY MATERIALS

Supplementary material for this article is available at http://advances.sciencemag.org/cgi/content/full/5/10/eaax5733/DC1

Fig. S1. Basic characterization of $PdCoO_2$ thin films grown on β-Ga_2O_3 (−201).

Fig. S2. Relationship between work function and lattice constant for typical metal electrodes with a (pseudo-)hexagonal lattice constant close to the representative hexagonal wide-gap semiconductors.

Fig. S3. Temperature dependence of the Schottky barrier height and the ideality factor.

Fig. S4. Determination of the work function for $PdCoO_2$ using the ultraviolet photoelectron spectroscopy.

Fig. S5. Stability of $PdCoO_2$ thin films in a harsh environment.

Table S1. Summary of the metal/β-Ga_2O_3 junctions reported in literature.

Table S2. Summary of the partially oxidized metal/β-Ga_2O_3 junctions reported in literature.

REFERENCES AND NOTES

1. B. J. Baliga, *Fundamentals of Power Semiconductor Devices* (Springer, 2008).
2. P. G. Neudeck, R. S. Okojie, L.-Y. Chen, High-temperature electronics—A role for wide bandgap semiconductors? *Proc. IEEE* **90**, 1065–1076 (2002).
3. S. M. Sze, K. K. Ng, *Physics of Semiconductor Devices* (Wiley, 2006).
4. J. Y. Tsao, S. Chowdhury, M. A. Hollis, D. Jena, N. M. Johnson, K. A. Jones, R. J. Kaplar, S. Rajan, C. G. van de Walle, E. Bellotti, C. L. Chua, R. Collazo, M. E. Coltrin, J. A. Cooper, K. R. Evans, S. Graham, T. A. Grotjohn, E. R. Heller, M. Higashiwaki, M. S. Islam, P. W. Juodawlkis, M. A. Khan, A. D. Koehler, J. H. Leach, U. K. Mishra, R. J. Nemanich, R. C. N. Pilawa-Podgurski, J. B. Shealy, Z. Sitar, M. J. Tadjer, A. F. Witulski, M. Wraback, J. A. Simmons, Ultrawide-bandgap semiconductors: Research opportunities and challenges. *Adv. Electron. Mater.* **4**, 1600501 (2018).
5. M. Higashiwaki, K. Sasaki, H. Murakami, Y. Kumagai, A. Koukitu, A. Kuramata, T. Masui, S. Yamakoshi, Recent progress in Ga_2O_3 power devices. *Semicond. Sci. Technol.* **31**, 034001 (2016).
6. E. Farzana, Z. Zhang, P. K. Paul, A. R. Arehart, S. A. Ringel, Influence of metal choice on (010) β-Ga_2O_3 Schottky diode properties. *Appl. Phys. Lett.* **110**, 202102 (2017).
7. K. Sasaki, M. Higashiwaki, A. Kuramata, T. Masui, S. Yamakoshi, Ga_2O_3 Schottky barrier diodes fabricated by using single-crystal β-Ga_2O_3 (010) substrates. *IEEE Electr. Device L.* **34**, 493–495 (2013).
8. T. Oishi, Y. Koga, K. Harada, M. Kasu, High-mobility β-Ga_2O_3 (−201) single crystals grown by edge-defined film-fed growth method and their Schottky barrier diodes with Ni contact. *Appl. Phys. Express* **8**, 031101 (2015).
9. K. Irmscher, Z. Galazka, M. Pietsch, R. Uecker, R. Fornari, Electrical properties of β-Ga_2O_3 single crystals grown by the Czochralski method. *J. Appl. Phys.* **110**, 063720 (2011).
10. J. Yang, S. Ahn, F. Ren, S. J. Pearton, S. Jang, J. Kim, A. Kuramata, High reverse breakdown voltage Schottky rectifiers without edge termination on Ga_2O_3. *Appl. Phys. Lett.* **110**, 192101 (2017).
11. S. Müller, H. von Wenckstern, F. Schmidt, D. Splith, F. L. Schein, H. Frenzel, M. Grundmann, Comparison of Schottky contacts on β-gallium oxide thin films and bulk crystals. *Appl. Phys. Express* **8**, 121102 (2015).
12. S. Müller, H. von Wenckstern, F. Schmidt, D. Splith, H. Frenzel, M. Grundmann, Method of choice for the fabrication of high-quality β-gallium oxide-based Schottky diodes. *Semicond. Sci. Technol.* **32**, 065013 (2017).
13. C. Hou, R. M. Gazoni, R. J. Reeves, M. W. Allen, Direct comparison of plain and oxidized metal Schottky contacts on β-Ga_2O_3. *Appl. Phys. Lett.* **114**, 033502 (2019).
14. W. M. Haynes, D. R. Lide, T. J. Bruno, *CRC Handbook of Chemistry and Physics 97th Edition* (CRC Press, 2017).
15. S. J. Pearton, F. Ren, M. Tadjer, J. Kim, Perspective: Ga_2O_3 for ultra-high power rectifiers and MOSFETS. *J. Appl. Phys.* **124**, 220901 (2018).
16. A. P. Mackenzie, The properties of ultrapure delafossite metals. *Rep. Prog. Phys.* **80**, 032501 (2017).
17. R. Daou, R. Frésard, V. Eyert, S. Hébert, A. Maignan, Unconventional aspects of electronic transport in delafossite oxides. *Sci. Technol. Adv. Mater.* **18**, 919–938 (2017).
18. H. Takatsu, S. Yonezawa, S. Mouri, S. Nakatsuji, K. Tanaka, Y. Maeno, Roles of high-frequency optical phonons in the physical properties of the conductive delafossite $PdCoO_2$. *J. Phys. Soc. Japan* **76**, 104701 (2007).
19. P. J. W. Moll, P. Kushwaha, N. Nandi, B. Schmidt, A. P. Mackenzie, Evidence for hydrodynamic electron flow in $PdCoO_2$. *Science* **351**, 1061–1064 (2016).
20. M. Tanaka, M. Hasegawa, T. Higuchi, T. Tsukamoto, Y. Tezuka, S. Shin, H. Takei, Origin of the metallic conductivity in $PdCoO_2$ with delafossite structure. *Physica B* **245**, 157–163 (1998).
21. V. Sunko, H. Rosner, P. Kushwaha, S. Khim, F. Mazzola, L. Bawden, O. J. Clark, J. M. Riley, D. Kasinathan, M. W. Haverkort, T. K. Kim, M. Hoesch, J. Fujii, I. Vobornik, A. P. Mackenzie, P. D. C. King, Maximal Rashba-like spin splitting via kinetic-energy-coupled inversion-symmetry breaking. *Nature* **549**, 492–496 (2017).
22. F. Mazzola, V. Sunko, S. Khim, H. Rosner, P. Kushwaha, O. J. Clark, L. Bawden, I. Marković, T. K. Kim, M. Hoesch, A. P. Mackenzie, P. D. C. King, Itinerant ferromagnetism of the Pd-terminated polar surface of $PdCoO_2$. *Proc. Natl. Acad. Sci. U.S.A.* **115**, 12956–12960 (2018).
23. T. Harada, A. Tsukazaki, A versatile patterning process based on easily soluble sacrificial bilayers. *AIP Adv.* **7**, 085011 (2017).
24. H. He, R. Orlando, M. A. Blanco, R. Pandey, E. Amzallag, I. Baraille, M. Rérat, First-principles study of the structural, electronic, and optical properties of Ga_2O_3 in its monoclinic and hexagonal phases. *Phys. Rev. B* **74**, 195123 (2006).
25. C. Fares, F. Ren, S. J. Pearton, Temperature-dependent electrical characteristics of β-Ga_2O_3 diodes with W Schottky contacts up to 500°C. *ECS J. Solid State Sci. Technol.* **8**, Q3007–Q3012 (2019).
26. M. J. Tadjer, V. D. Wheeler, D. I. Shahin, C. R. Eddy Jr., F. J. Kub, Thermionic emission analysis of TiN and Pt Schottky contacts to β-Ga_2O_3. *ECS J. Solid State Sci. Technol.* **6**, 165–168 (2017).
27. D. Splith, S. Müller, F. Schmidt, H. von Wenckstern, J. J. van Rensburg, W. E. Meyer, M. Grundmann, Determination of the mean and the homogeneous barrier height of Cu Schottky contacts on heteroepitaxial β-Ga_2O_3 thin films grown by pulsed laser deposition. *Phys. Status Solidi* **211**, 40–47 (2014).
28. J. Yang, F. Ren, S. J. Pearton, A. Kuramata, Vertical geometry, 2-A forward current Ga_2O_3 Schottky rectifiers on bulk Ga_2O_3 substrates. *IEEE Trans. Electron Devices* **65**, 2790–2796 (2018).
29. M. Higashiwaki, K. Konishi, K. Sasaki, K. Goto, K. Nomura, Q. T. Thieu, R. Togashi, H. Murakami, Y. Kumagai, B. Monemar, A. Koukitu, A. Kuramata, S. Yamakoshi, Temperature-dependent capacitance–voltage and current–voltage characteristics of Pt/Ga_2O_3 (001) Schottky barrier diodes fabricated on n^--Ga_2O_3 drift layers grown by halide vapor phase epitaxy. *Appl. Phys. Lett.* **108**, 133503 (2016).
30. K. Konishi, K. Goto, H. Murakami, Y. Kumagai, A. Kuramata, S. Yamakoshi, M. Higashiwaki, 1-kV vertical Ga_2O_3 field-plated Schottky barrier diodes. *Appl. Phys. Lett.* **110**, 103506 (2017).
31. F. Ren, J. C. Yang, C. Fares, S. J. Pearton, Device processing and junction formation needs for ultra-high power Ga_2O_3 electronics. *MRS Commun.* **9**, 77–87 (2019).
32. M. Mohamed, K. Irmscher, C. Janowitz, Z. Galazka, R. Manzke, R. Fornari, Schottky barrier height of Au on the transparent semiconducting oxide β-Ga_2O_3. *Appl. Phys. Lett.* **101**, 132106 (2012).
33. J. Rogal, K. Reuter, M. Scheffler, Thermodynamic stability of PdO surfaces. *Phys. Rev. B* **69**, 075421 (2004).
34. T. Yajima, Y. Hikita, M. Minohara, C. Bell, J. A. Mundy, L. F. Kourkoutis, D. A. Muller, H. Kumigashira, M. Oshima, H. Y. Hwang, Controlling band alignments by artificial interface dipoles at perovskite heterointerfaces. *Nat. Commun.* **6**, 6759 (2015).
35. T. Harada, K. Fujiwara, A. Tsukazaki, Highly conductive $PdCoO_2$ ultrathin films for transparent electrodes. *APL Mater.* **6**, 046107 (2018).
36. H. Hoeneisen, C. A. Mead, M.-A. Nicolet, Permittivity of β-Ga_2O_3 at low frequencies. *Solid-State Electron.* **14**, 1057–1059 (1971).
37. J. H. Werner, H. H. Güttler, Barrier inhomogeneities at Schottky contacts. *J. Appl. Phys.* **69**, 1522–1533 (1991).
38. G. Jian, Q. He, W. Mu, B. Fu, H. Dong, Y. Qin, Y. Zhang, H. Xue, S. Long, Z. Jia, H. Lv, Q. Liu, X. Tao, M. Liu, Characterization of the inhomogeneous barrier distribution in a Pt/(100) β-Ga_2O_3 Schottky diode via its temperature-dependent electrical properties. *AIP Adv.* **8**, 015316 (2018).

Acknowledgments: This work is a cooperative program (proposal no. 16G0404) of the CRDAM-IMR, Tohoku University. We thank the NEOARK Corporation for lending a mask-less lithography system PALET. **Funding:** This work was supported, in part, by a Grant-in-Aid for Specially Promoted Research (no. 25000003), a Grant-in-Aid for Scientific Research (A) (no. 15H02022), and a Grant-in-Aid for Early-Career Scientists (no. 18K14121) from the Japan Society for the Promotion of Science (JSPS), JST CREST (JPMJCR18T2), the Mayekawa Houonkai

Foundation, and the Tanaka Foundation. **Author contributions:** T.H. and A.T. designed the experiments. T.H. prepared the samples, performed transport measurements, and analyzed the data. S.I. captured the HAADF-STEM image. T.H. and A.T. wrote the manuscript. **Competing interests:** The authors declare that they have no competing interests. **Data and materials availability:** All data needed to evaluate the conclusions in the paper are present in the paper and/or the Supplementary Materials. Additional data related to this paper may be requested from the authors.

Submitted 3 April 2019
Accepted 25 September 2019
Published 18 October 2019
10.1126/sciadv.aax5733

Citation: T. Harada, S. Ito, A. Tsukazaki, Electric dipole effect in $PdCoO_2/\beta\text{-}Ga_2O_3$ Schottky diodes for high-temperature operation. *Sci. Adv.* **5**, eaax5733 (2019).